PERGAMON

Radiation Measurements 35 (2002) 457–471

Radiation Measurements

www.elsevier.com/locate/radmeas

Passive dosimetry aboard the Mir Orbital Station: external measurements

E.R. Benton[a,*], E.V. Benton[b], A.L. Frank[b]

[a] *Eril Research, Inc., P.O. Box 150788, San Rafael, CA 94915-0788, USA*
[b] *University of San Francisco, 2130 Fulton St., San Francisco, CA 94117-1080, USA*

Received 1 April 2002

Abstract

This paper reports results from the first measurements made on the exterior of a LEO spacecraft of mean dose equivalent rate and average quality factor as functions of shielding depth for shielding less than 1 g/cm^2 A1 equivalent. Two sets of measurements were made on the outside of the Mir Orbital Station; one near solar maximum in June 1991 and one near solar minimum in 1997. Absorbed dose was measured using stacks of TLDs. LET spectrum from charged particles of $LET_\infty H_2O \geqslant 5$ keV/μm was measured using stacks of CR-39 PNTDs. Results from the TLD and PNTD measurements at a given shielding depth were combined to yield mean total dose rate, mean dose equivalent rate, and average quality factor. Measurements made near solar maximum tend to be greater than those made during solar minimum. Both mean dose rate and mean dose equivalent rate decrease by nearly four orders of magnitude within the first g/cm^2 shielding illustrating the attenuation of both trapped electrons and low-energy trapped protons. In order to overcome problems with detector saturation after standard chemical processing, measurement of LET spectrum in the least shielded CR-39 PNTD layer (0.005 g/cm^2 A1) was carried out using an atomic force microscope.

1. Introduction

The ionizing radiation environment present on the exterior of low-Earth orbit (LEO) spacecraft differs considerably from that encountered within the habitable interior of the spacecraft. The electron and low-energy trapped and galactic cosmic ray (GCR) proton components in open space are almost completely attenuated by the outer skin and structure of the spacecraft. This attenuation results in orders-of-magnitude larger dose rates on the exterior versus the interior of LEO spacecraft and a steep dose gradient within the first g/cm^2 of spacecraft shielding. Interactions between protons and heavy ions with the mass of the spacecraft produce fluxes of secondary neutrons and charged particles in the interior of LEO spacecraft which, for the most part, are not present in open space.

The unprecedented level of EVA required for the assembly of the International Space Station (ISS) has led to a recognition of the importance of radiation dosimetry on the exterior of LEO spacecraft, especially during EVA. At the completion of the ISS on-orbit assembly, space crews will have accumulated nearly 1000 EVA hours—over two and a half times the total number of EVA hours accrued by all astronauts and cosmonauts to date (NASA, 2001). A program of testing the radiation shielding properties of US and Russian EVA suits has been carried out at ground-based accelerators (Cucinotta, 2001; Benton et al., 2001b). However, while extensive measurements have been made of the space radiation environment within the habitable volume of piloted spacecraft such as the NASA Space Shuttle, the Russian Mir Orbital Station and the ISS using both active and passive detectors, relatively few dosimetric measurements have been conducted on the exterior of such spacecraft (Benton and Benton, 2001a; Deme et al., 1999).

* Corresponding author.
E-mail address: eric@erilresearch.com (E.R. Benton).

1350-4487/02/$ - see front matter
PII: S1350-4487(02)00076-8

The main objectives of the few external radiation measurements that have been made in LEO have tended to focus on the effects of ionizing radiation on materials such as radiation sensitive electronics and optical coatings or on validating environment models (Dyer et al., 1999; Bühler et al., 1996). A fairly large number of measurements of dose as a function of shielding depth for depths less than 1 g/cm^2 have been carried out on the exterior of LEO spacecraft using stacks of TLDs (Benton and Benton, 1999). These measurements have been made by a number of different laboratories, including that of the authors, mostly aboard Russian recoverable satellites (Akatov et al., 1986; Charvat et al., 1990; Schmidt et al., 1990; Akatov et al., 1990; Spurny and Votochkova, 1992; Szabo et al., 1986). In this paper, we present results from the first measurements of dose equivalent and average quality factor as a function of shielding depth made on the exterior of a piloted spacecraft.

During the operational lifetime of the Mir Orbital Station, we carried out two separate measurements of dose and dose equivalent external to the Mir using passive detectors. The first experiment was conducted during a 28-day period in June, 1991 near solar maximum. The second experiment was carried out over a 130-day period in mid-1997, encompassing solar minimum. Two types of passive radiation detector were employed. Stacks of TLDs, similar to those used in previous dose/depth measurements made aboard recoverable Russian satellites (Benton and Benton, 1999), were used to measure absorbed dose as a function of shielding depth at shielding depths between 0.015 and 3.20 g/cm^2 A1. Hermetically sealed stacks of CR-39 plastic nuclear track detector (PNTD) were used to measure the LET spectrum from charged particles of $LET_\infty H_2O \geqslant 5$ keV/μm at shielding depths between 0.005 and 5.5 g/cm^2 A1. Results from the TLD dose measurements and CR-39 PNTD LET spectrum measurements were then combined to yield mean total dose rate, dose equivalent rate, and average quality factor as functions of shielding depth.

Following conventional chemical processing, the least-shielded (0.005 g/cm^2 A1) layer of CR-39 in the 1997 experiment was saturated with overlapping particle tracks and the LET spectrum could not be measured using an optical microscope. This was due to the high flux of low-energy protons at this shielding depth. A second PNTD layer, exposed at the same shielding depth, was processed for a significantly shorter period of time and the LET spectrum was measured using a new technique—atomic force microscopy (AFM). We believe that this result represents the first reporting of an LET spectrum measurement made in nuclear track detector using AFM and is the least-shielded LET spectrum measurement made in space using passive detectors to date. AFM offers a unique capability to analyze track detectors exposed to extremely high ($> 10^8$ cm^{-2}) charged particle fluences.

2. Experiment

2.1. Exposure configuration

To measure the space radiation environment on the exterior of the Mir Orbital Station, we used two types of passive radiation detector. Thermoluminescent detectors (TLDs) were used to measure absorbed dose. CR-39 PNTDs were used to measure the mean LET flux, dose rate and dose equivalent rate spectra from charged particles of $LET_\infty H_2O \geqslant 5$ keV/μm. Stacks of both types of detector were arrayed in such a way that the relevant quantities could be measured as a function of position within the detector stack. Subsequently, position within the detector stack was converted to shielding depth in Al in the vertical direction. TLD results were combined with the results from the CR-39 PNTDs at the discrete shielding depths at which the PNTD measurements were made yielding mean total dose rate, dose equivalent rate, and average quality factor as functions of shielding depth in Al.

Both the 1991 and 1997 external experiments were made using the STD platform on the exterior of the Kvant 2 module, near the main EVA airlock. The STD platform was a metal frame mounted above the two upper gyrodynes approximately halfway along the length of the Kvant 2 module, as pictured in Fig. 1. The passive detectors were mounted on an aluminum experiment tray, which in turn was attached to the STD platform via a spring-loaded locking mechanism. The experiment tray and mounted detector stacks were collectively referred to as the External Dosimeter Array (EDA). The EDA used in the 1997 experiment is pictured in Fig. 2. The EDA was deployed to and retrieved from the STD platform by the cosmonauts during EVA.

Each TLD stack consisted of approximately 22 thin (0.091 mm) and 15 thick (0.89 mm) TLD-700 (^{7}LiF) chips mounted in a cylindrical Lexan holder. The Lexan holder was covered by a thin (15 μm) layer of aluminized Kapton that provided protection with a minimum of shielding. Two TLD stacks were then mounted in an Al block that was in turn mounted on the EDA platform.

The CR-39 PNTDs took the form of 3.33 cm diameter disks stacked in Al canisters. In the 1991 experiment, six layers of 600 μm thick CR-39, separated by layers of 8 μm thick polycarbonate foil, were placed in each canister and two such canisters were mounted one atop the other. Approximately 2 mm A1 separated the least-shielded PNTD layer from space while a thickness of 12 mm A1 separated the PNTD layers in the two canisters. In the 1997 experiment, each canister contained approximately 16 layers of 600 μm thick CR-39, separated by layers of 8 μm thick polycarbonate foil. Two Al canisters were exposed side by side. The top of each Al canister was open to space except for two layers of Aluminized Kapton film. The Kapton film served to maintain the air environment inside the canisters and to protect the PNTD stacks during handling. Because CR-39 must be in the presence of oxygen to function properly, the

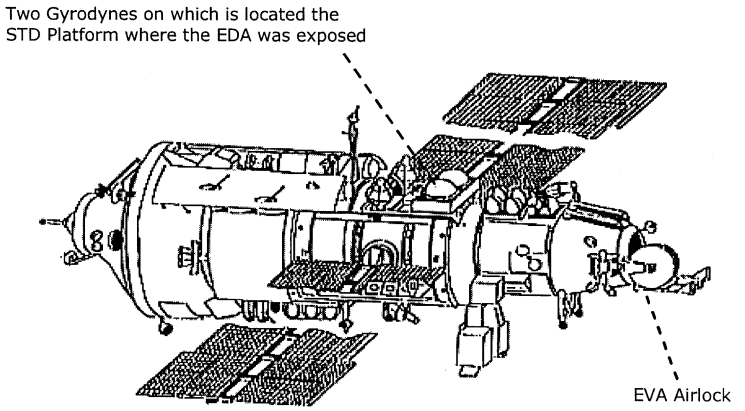

Fig. 1. Location of the STD platform on the exterior of the Kvant 2 module.

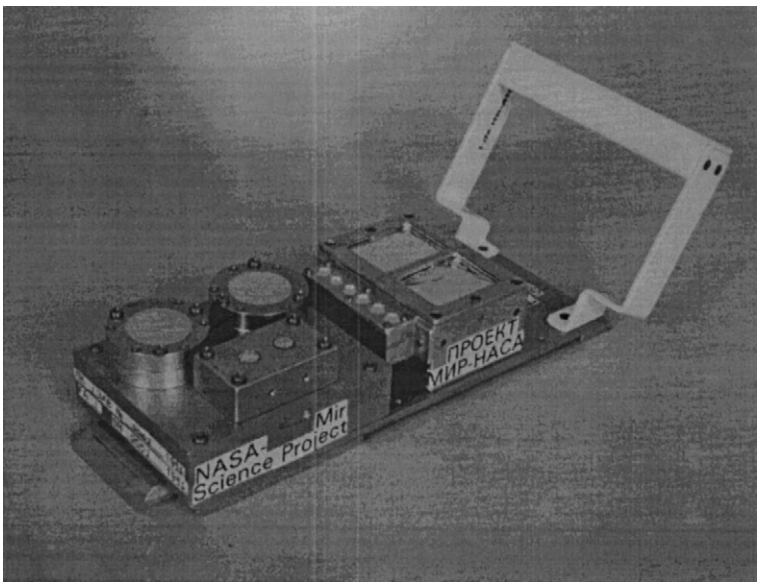

Fig. 2. EDA exposed in 1997 during solar minimum. US detectors are at the front, Russian detectors are next to the handle.

capsules were hermetically sealed using rubber o-rings. The sealed capsules were then attached to the EDA platform.

The configuration and location of the STD platform on the outside of the Kvant 2 module required that the EDA design be completely passive and no temperature control or active temperature monitoring was possible. A thermal analysis of the EDA carried out during hardware flight certification indicated that there was strong thermal coupling between the STD platform and the rest of the Kvant 2 module and that the temperature of the EDA during external deployment was not expected to drop below -65°C or exceed 54°C during the course of the exposure. Several passive temperature sensors were incorporated into the EDA, the results from which indicated that the temperature never exceeded 40°C.

2.2. Exposure chronology

The first EDA and the Mir-9 APD were delivered to Mir by Soyuz TM-12 on 19 May 1991. The EDA was deployed to the STD platform on the exterior of the Kvant 2 module on 24 June during the first Mir-9 EVA by cosmonauts Anatoli Artseborski and Sergei Krikalev. The external exposure of the EDA lasted 33 days until it was retrieved during the sixth Mir-9 EVA on 27 July. The EDA was then stored on the interior of the Mir station until 11 October 1991, when it was returned to Earth along with the Mir-9 APD aboard Soyuz TM-12. The total duration of the mission was 145 days.

The second EDA was delivered to Mir during the STS-81 Space Shuttle mission. On 29 April 1997, the EDA was

deployed during EVA by US astronaut Jerry Linenger and Russian cosmonaut Anatoli Tsebliev. It was retrieved during the EVA of astronaut Mike Foale and cosmonaut Anatoli Solovyov on 5 September 1997. The EDA was returned to Earth by STS-86 on 5 October 1997 at the conclusion of the NASA-5 mission.

Prior to external deployment and following retrieval of the 1997 EDA from the STD platform, it was stored in the heavily shielded Ceiling Panel No. 303 location inside the Kvant 2 module. This location in the interior of the Kvant 2 module roughly corresponds to the external location of the STD platform near the airlock of the Kvant 2 as illustrated in Fig. 1. Ceiling Panel No. 303 was also the location of APD-6, which served as an internal control during the external exposure of the EDA. The total external exposure of the EDA lasted 130.1 days while its total time aboard Mir lasted 267.2 days (NASA-4/Mir-23 and NASA-5/Mir-24 missions).

2.3. Detector readout and analysis

The TLD dose rate was determined for each depth where a CR-39 PNTD LET spectrum was measured based on a polynomial fit to the TLD dose/depth measurements. Depth in LiF in the case of the TLD measurements and depth in CR-39 for the PNTD measurements were converted to equivalent depth in aluminum. The two dose rate values for each exposure were averaged for each measured shielding depth and a fourth-order polynomial was fitted to the averaged dose values. Uncertainty of each TLD dose measurement was taken to be 10%. From the fitted polynomial, the TLD dose rate was either interpolated or extrapolated for each PNTD depth.

LET spectrum was read out at five shielding depths in the 1991 EDA exposure and at six shielding depths in the 1997 EDA exposure. Chemical processing of the 1991 PNTD layers was in 50°C 6.25 N NaOH for 168 h. For five of the six 1997 detectors (excluding the least-shielded detector), each of the PNTD layers was cut in half. Both halves were etched in 50°C 6.25 N NaOH, one half for 36 h to enhance the short-range secondary component and one half for 168 h to enhance the lower-LET component. The detectors were then read out using an ELBEK Samaica track detector analysis system. Details of the detector readout and analysis of the two-etch-duration detectors from the 1997 exposure can be found in a companion paper in this issue (Benton et al., 2002).

Because the least-shielded layer of CR-39 was under only 0.005 g/cm^2 Al equivalent shielding, the fluence of particles was expected to be extremely high. In order to maintain small track size, thereby minimizing the amount of track overlap, chemical processing of the uppermost layer was originally carried out for only 24 h. Following chemical processing, the uppermost layer of CR-39 was found to be saturated with tracks. Fig. 3 shows photomicrographs of four CR-39 layers from the 1997 EDA CR-39 stack. All photomicrographs are at a magnification of 600×.

The photo in the upper left of Fig. 3 is from the least-shielded detector layer. The granulated appearance of the surface surrounding the pointed track is caused by overlapping tracks from stopping protons. Because the tracks are overlapping, it was not possible to measure the LET spectrum since the track perimeters could not be discerned. The photomicrograph in the upper right corner of Fig. 3 is of the second layer of CR-39. While there is still a high density of shallow tracks from stopping particles, the tracks no longer overlap and it is possible to make out their perimeters and accurately measure them. The two bottom photomicrographs in Fig. 3 are from the fourth and eighth layers, respectively. Here the track density was quite low and no longer appeared to be changing as a function of depth. The tracks visible in the bottom two photomicrographs are from both primary charged particles and stopping secondary particles.

In order to measure the LET spectrum in the least-shielded PNTD layer in the second 1997 EDA CR-39 PNTD stack, it was determined that the duration of the chemical etch must be significantly shorter than the 24 h etch of the least-shielded layer from the first PNTD stack. Because optical microscopy cannot resolve the small track sizes resulting from such a short duration etch, a new method for measuring the track perimeters was sought. AFM was determined to be the best solution. AFM is a mechanical means by which the topography of a surface may be imaged with nanometer resolution. Details of the use of AFM in analyzing PNTDs may be found in Yamamoto et al., 1999.

Fig. 4 shows an example of an AFM image of the surface of the least-shielded layer from the second PNTD stack after 4 h etch in 50°C 6.25 N NaOH. Each image or field of view of an etched CR-39 PNTD obtained by the AFM is the result of a 512 line, 512 sample points per line, scan of the detector surface by the scanner controlled cantilever probe. The bulk etch (thickness of bulk detector removed by chemical etching) was measured using the epoxy-mask technique developed by Yasuda et al. (1998) and found to be $\sim$ 0.84 μm. The detector surface was analyzed using a Digital Instruments DI-3100 AFM operating in tapping mode. Image size was 5 μm × 5 μm. The major and minor axes of the elliptical openings of the etched particle tracks were measured manually in the acquired image using the section tool in the DI Nanoscope III software. A detector response function based on multiple heavy ion exposures at ground-based particle accelerators was also measured using AFM. The response function was then used to convert the measured track values from the space-exposed detector to values of LET, which were used to determine an LET spectrum.

Because the EDAs were stored within the interior of Mir both prior to and following exposure on the exterior of Mir, the detectors received a significant exposure while inside the spacecraft in addition to that received while outside. A subtraction of the internal exposure was carried out using LET

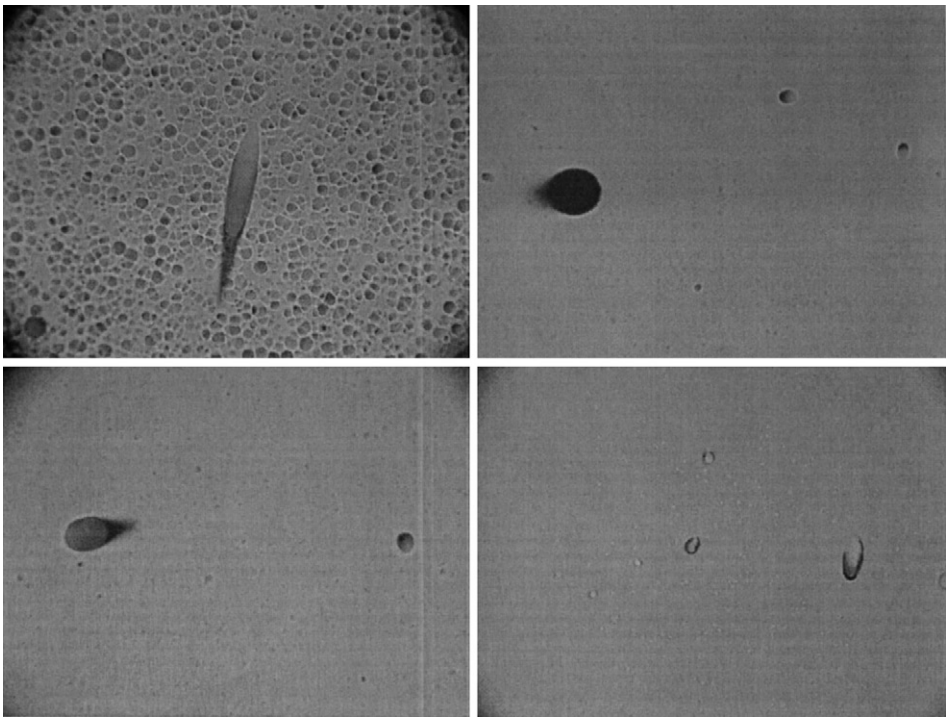

Fig. 3. Photomicrographs of CR-39 track detectors exposed on the EDA during the NASA-4/Mir-23 and NASA-5/Mir-24 missions. Clockwise starting in the upper left is the first, second, fourth and eighth layers. The first, top most layer was processed for 24 h while the other three layers were processed for 36 h. All photomicrographs were taken at a magnification of 600×.

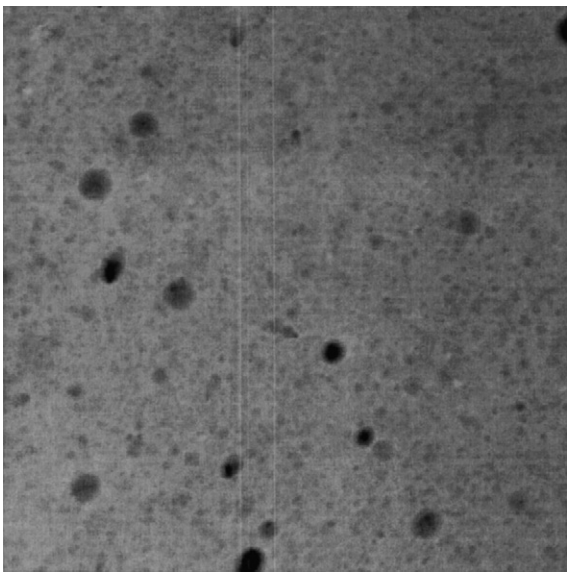

Fig. 4. AFM image of CR-39 PNTD exposed under 0.005 g/cm^2 on the exterior of the Mir in 1997. The size of the image is 5 μm × 5 μm.

spectra measured for the entire duration of the same mission inside Mir. For the 1997 experiment, an area passive dosimeter, APD-6, was exposed within the Kvant 2 module at a location near the STD platform. Before and after the external exposure, the 1997 EDA was stored in this same location. A differential LET fluence spectrum based on the APD-6 flux spectrum multiplied by the length of time the EDA was stored on the interior of the Kvant 2 module was subtracted from the total differential LET fluence spectra measured in each EDA PNTD layer. The resulting fluence spectra were then divided by the length of the external exposure in order to obtain the external mean flux spectra. The duration of the 1997 external exposure was 130.1 days while the total duration the 1997 EDA was stored inside the Kvant 2 module prior to and following the external exposure was 137.4 days. A similar procedure was carried out for the 1991 EDA. However, the length of the 1991 EDA exposure was only 33 days, while the length of time the 1991 EDA was stored on the interior of Mir was 112 days. In performing a subtraction of the internal exposure in this way, an assumption is made that the flux over the entire length of the experiment is, more or less, constant. While this is likely to be the case for the 1997 exposure carried out under solar minimum conditions, there were a number of large solar particle events during the 1991 mission during both the time the EDA was stored

inside Mir and during the external exposure. In addition, the EDA was not stored in the same location as the APD during the 1991 mission so that the shielding of the two internal exposures was not the same. However, given the nature of the passive detectors, there was little alternative but to use this assumption.

Mean total dose rate, dose equivalent rate and average quality factor were measured at each shielding depth where a PNTD layer was analyzed. Dose rate, dose equivalent rate and average quality factor was determined using the LET dose rate and dose equivalent rate spectra $\geqslant 5$ keV/μm measured in CR-39 PNTDs and including a subtraction of the internal exposure, and interpolated TLD dose rates from the dose/depth profiles. The procedure for determining mean total dose rate, dose equivalent rate and average quality factor is described in detail in a companion paper published in this issue (Benton et al., 2002). The ICRP-60 (ICRP, 1991) definition of quality factor was used in determining dose equivalent.

3. Results and discussion

3.1. Dose/depth measurements in TLD

Results from the dose/depth measurements made in the TLD stacks are shown in Fig. 5. The two upper curves show dose rate as a function of shielding depth in aluminum measured on the exterior of Mir in 1991. The two lower curves in Fig. 6 show similar measurements carried out in 1997. For both experiments there is an approximately three order of magnitude decrease in dose rate with in the first g/cm^2 of Al equivalent shielding. In the 1991 measurements, dose rate decreased from between 300 and 400 cGy/day

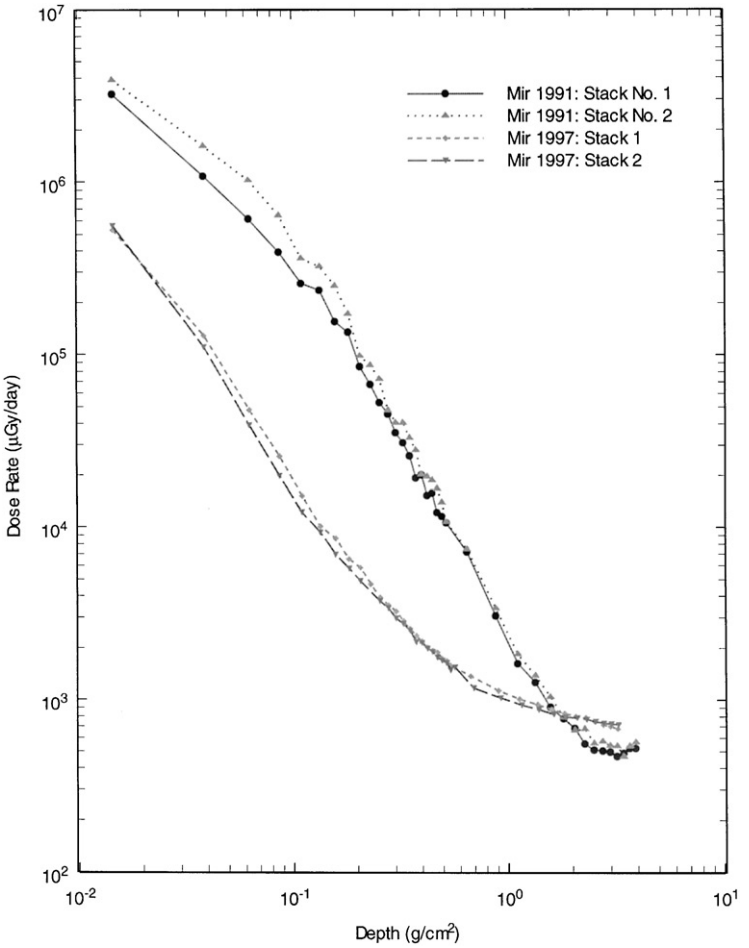

Fig. 5. Absorbed dose rate as a function of depth in Al measured in TLD stacks exposed on the exterior of Mir in 1991 near solar maximum and in 1997 following solar minimum.

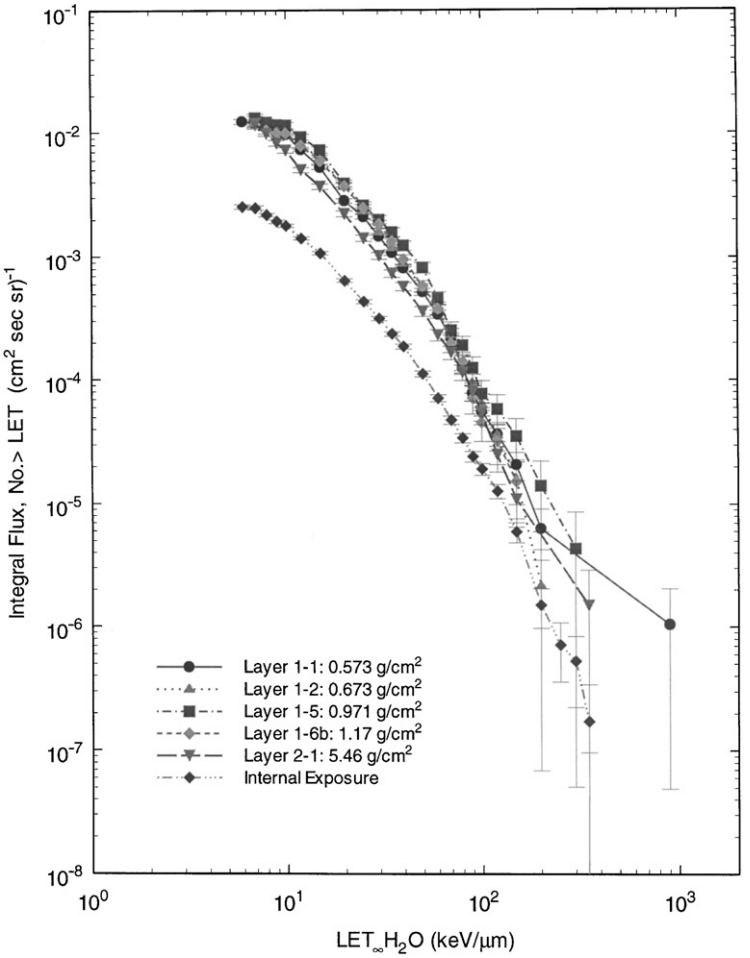

Fig. 6. Integral LET flux spectra measured on the exterior of the Mir Kvant 2 module in 1991 near solar maximum. Internal subtraction is not included.

under 0.015 g/cm^2 to less than 0.2 cGy/day at 1 g/cm^2. Similarly in the 1997 measurement, dose rate decreased from between 50 and 60 cGy/day under 0.015 g/cm^2 to approximately 0.1 cGy/day under 1 g/cm^2 of Al equivalent shielding.

In Fig. 5, shielding depth is taken to be only the vertical depth straight down through the TLD stack. Up to $\sim$ 1 g/cm^2, this direction possesses significantly less shielding than any other direction. After 1 g/cm^2, the shielding in the vertical direction begins to be comparable to that in the other directions, especially to the sides, and this is one reason why the curves tend to level off at depths in excess of 1 g/cm^2.

The two major contributors to dose at shielding depths less than 1 g/cm^2 are electrons encountered in the horns of the trapped electron belt at high latitudes and protons trapped in the South Atlantic Anomaly. The majority of trapped electrons are of energy less than 5 MeV and are thus attenuated within the first g/cm^2. The trapped electron flux in LEO is greater during solar maximum than during solar minimum (Stassinopoulos, 1988), so the fact that the 1991 measurements lie above the 1997 measurements is to be expected. Trapped proton flux in LEO is greater during solar minimum than during solar maximum when the increased solar wind ionizes the uppermost layers of the atmosphere leading to an increase in the atmospheric scale height. Increased atmospheric scale height translates into greater attenuation of the trapped proton flux at a given altitude.

During the time the 1991 external exposure was made, there were a number of large solar particle events and, in particular, a large event occurred on 9 June 1991. This event led to an increase in the dose rate from protons on the interior of Mir as measured using the Liulin portable spectrometer (Dachev et al., 1999) and the R-16 operational dosimeter (Mitrikas and Tsetlin, 1995). The additional proton flux from this event is included in our 1991 depth/dose

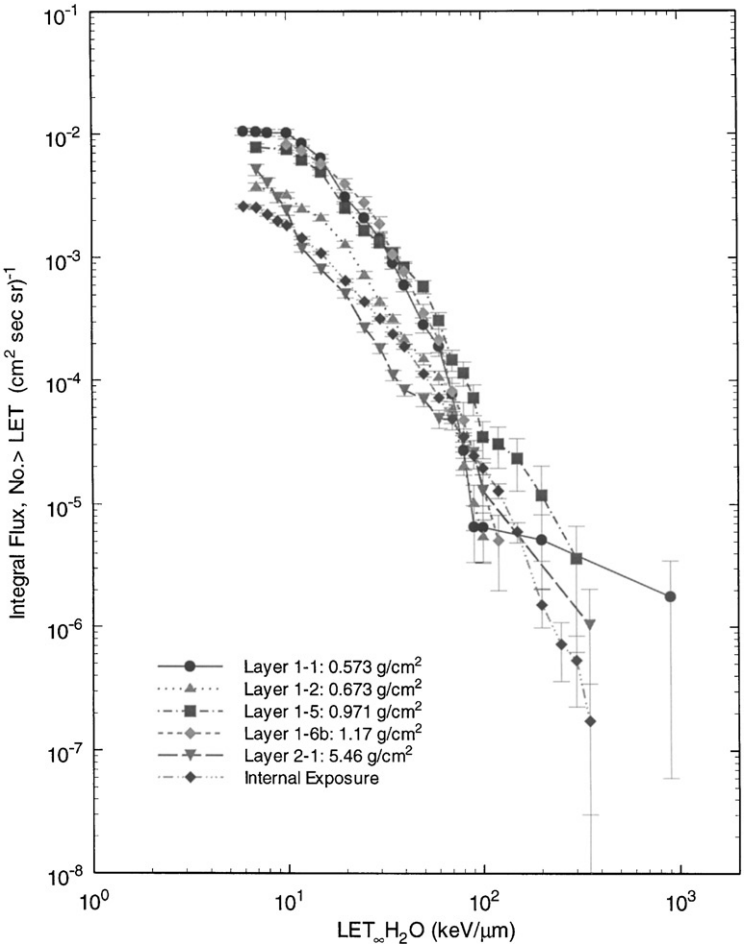

Fig. 7. Integral LET flux spectra measured on the exterior of the Mir Kvant 2 module in 1991 near solar maximum. Includes subtraction of internal exposure.

measurements. Additional dose also came from the passage of the Mir through the temporary trapped proton belt created in the slot region between $L = 2$ and 2.5 by the 24 March 1991 SPE (Gussenhoven et al., 1996; Shea and Smart, 1996).

3.2. LET spectrum measurements in CR-39 PNTDs

The integral LET flux spectra $\geqslant 5$ keV/μm measured at five shielding depths in the 1991 EDA are shown in Fig. 6. Also shown in Fig. 6 is the LET spectrum measured in the APD exposure during the same time period on the inside of Mir and used in making the subtraction of the internal contribution to the EDA exposure. There is fairly close agreement between all the external LET spectra below 100 keV/μm, with the exception of the spectrum measured in Layer 2–1. Above 100 keV/μm, the differences in the external spectra are likely a result of low statistics arising from the fact that relatively few high LET particle tracks were measured.

Fig. 7 shows the 1991 EDA LET spectra following subtraction for the internal contribution. There is no longer good agreement amongst the externally measured spectra, nor is there any discernible trend of a decrease in the spectra with increasing shielding, even at low LET. Furthermore, the internal subtraction has resulted in distorting the smooth shape of the curve that is typically seen in integral LET spectrum measurements made in LEO. The assumptions and limitations inherent in the procedure used in performing the internal subtraction are undoubtedly responsible for this poor result. As mentioned above, the duration of the internal exposure was over three times that of the external exposure. This fact may explain much of the good agreement in the external spectrum before internal subtraction. Given the large amount of solar activity during the Mir-9 mission, the assumption that the incident proton flux was fairly constant

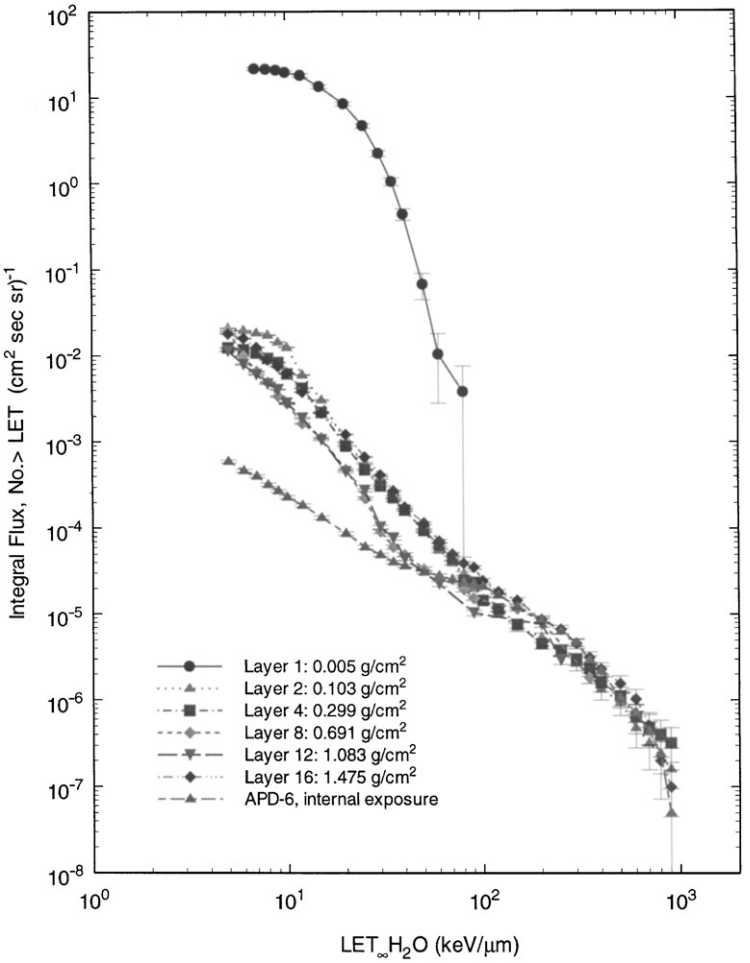

Fig. 8. Internal LET flux spectrum measured on the exterior of the Mir Kvant 2 module in 1997 following solar minimum. Internal subtraction is not included.

is not valid. Since the APD and EDA were not exposed in the same location while both dosimeters were on the interior of Mir, shielding conditions were different and the use of the APD data in making the internal subtraction is also not strictly valid. Moreover, it is probable that the Mir-9 APD was moved to a different exposure location inside Mir midway through the mission, so its shielding environment was not constant. Despite these limitations, there was no other means by which the internal contribution to the EDA could be separated from that made while the EDA was exposed on the outside of Mir.

Fortunately the problems present in the 1991 EDA LET spectra are largely absent in the LET spectrum measurements made in the 1997 EDA detectors. Because the 1997 EDA exposure took place during solar minimum, there was little solar activity and the incident particle flux remained fairly constant. In addition, great care was taken to ensure that APD-6 was exposed under the same shielding condition while both the EDA and APD were on the interior of Mir and that APD-6 was not moved during the mission.

Fig. 8 shows the mean integral LET flux spectra measured at six shielding depths in the 1997 EDA. Also shown in Fig. 8 is the integral LET flux spectrum measured in APD-6, which was exposed during the same time and at the same location on the inside of the Kvant 2 as the EDA detectors. By far the most obvious feature in Fig. 8 is that the spectrum measured in the least shielding detector (under 0.005 g/cm^2 and analyzed using AFM) lies fully three orders of magnitude above the remaining five spectra. This illustrates the attenuation of the trapped proton flux within the first 0.1 g/cm^2. Note that electrons do not produce particle tracks in CR-39 PNTD and nearly all the tracks measured in Layer 1 are from protons of energy < 14 MeV (Ogura et al., 1986).

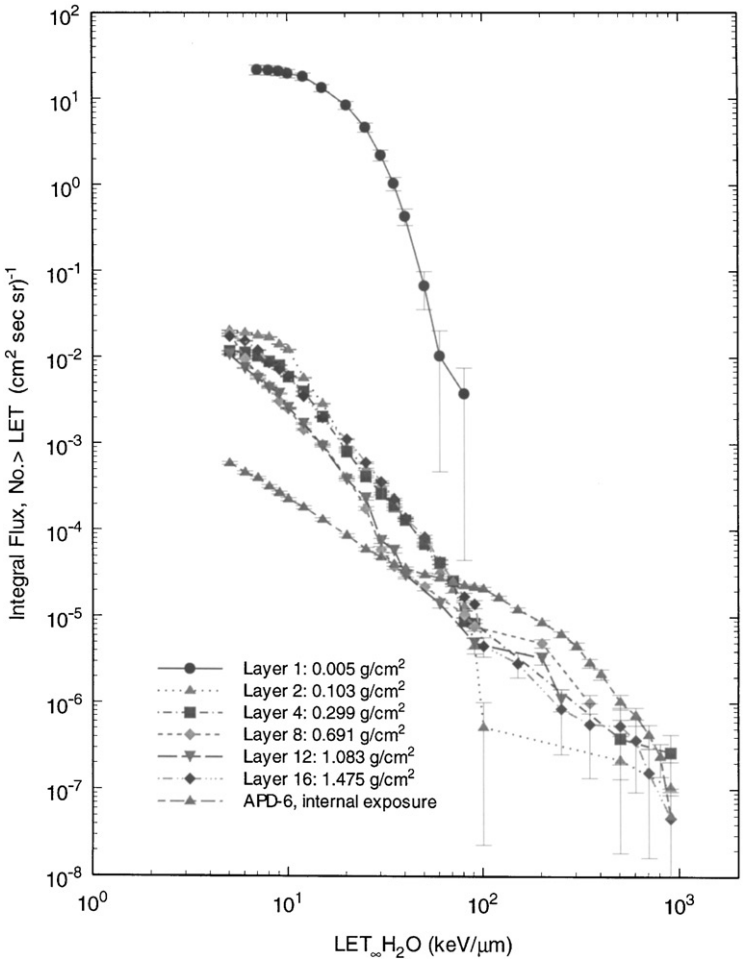

Fig. 9. Integral LET flux spectrum measured on the exterior of the Mir Kvant 2 module in 1997 following solar minimum. Includes subtraction of internal exposure.

The agreement in the LET spectra measured in Layers 2–16 in Fig. 8 is quite close and, with the exception of the spectrum measured in Layer 16, the expected decrease in LET spectrum with increased shielding can be seen below 100 keV/μm. Above 100 keV/μm, agreement remains close; however, there is also close agreement with the spectrum measured in the internal APD-6 detector.

Fig. 9 shows the integral LET flux spectra measured in the 1997 EDA following subtraction of the internal exposure. The EDA spectra below 100 keV/μm remain little changed, but above 100 keV/μm there is a substantial reduction in the spectra following internal subtraction. This indicates that the majority of tracks from particles of LET $>$ 100 keV/μm were due to the internal exposure of the EDA. Most of these high LET particles are short-range recoils and particles of $Z = 2$ produced by proton and neutron interactions with shielding in the form of the spacecraft and its contents, including the detector itself (see Benton et al., 2002).

3.3. Combined TLD and PNTD results

Figs. 10 and 11 show the mean total dose rate and dose equivalent rate, respectively, from the combined TLD and CR-39 PNTD measurements as functions of Al equivalent shielding depth for both the 1991 and 1997 EDA exposures. Tables 1 and 2 show the tabulated results for total dose rate, dose equivalent rate and average quality factor for the 1991 and 1997 EDA exposures, respectively. Also shown in Tables 1 and 2 are the uncorrected dose rates interpolated from the TLD stacks and the dose and dose equivalent rates from particles of LET $\geqslant$ 10 keV/μm. Both mean dose rate and dose equivalent rate decrease by nearly four orders of magnitude within the first g/cm^2 of shielding in the 1997 measurements. Because all the measurements made in the

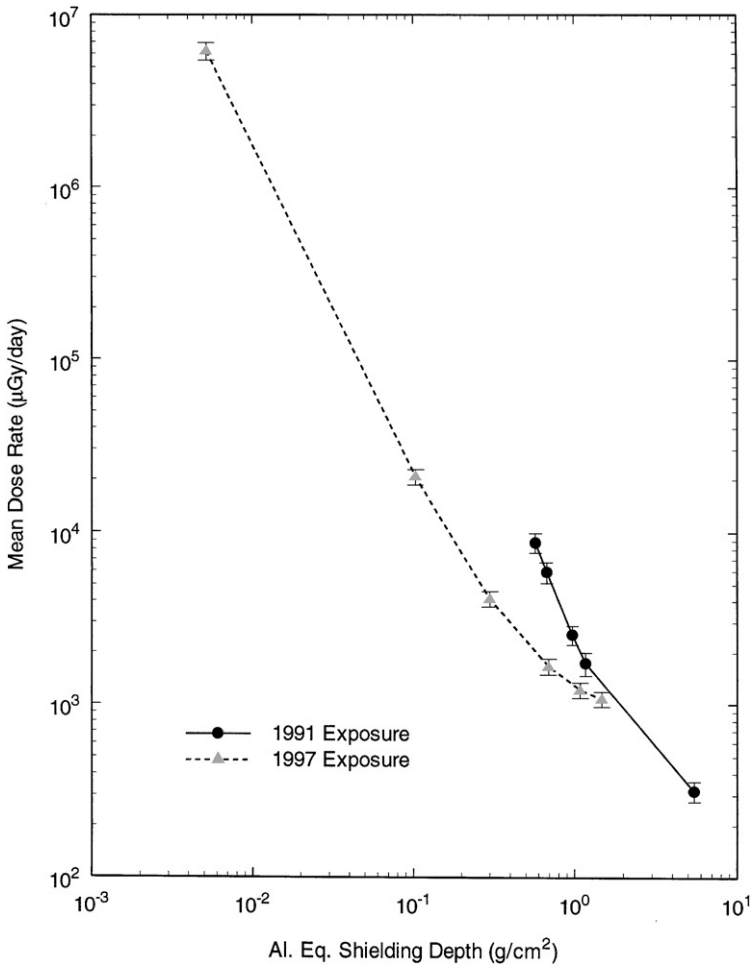

Fig. 10. Mean total dose rate as a function of shielding depth in Al measured on the exterior of the Mir Kvant 2 module in 1991 and 1997.

1991 EDA were under considerably greater shielding, the decrease in mean dose rate and dose equivalent rate is not nearly so dramatic. However, as in the dose/depth profiles measured in the TLD stacks (Fig. 5), the results from the 1991 measurements lie above those made in 1997 for a given shielding depth.

Average quality factor as a function of Al equivalent shielding depth is shown in Fig. 12. In the 1991 measurements, there is a steady increase in average quality factor with shielding depth from approximately 1 under 0.57 g/cm^2 to nearly 4 under 5.5 g/cm^2. The reason for the speciously high-quality factor in the 5.5 g/cm^2 measurement is not known, but probably lies in the various limitations and assumptions inherent in the method described above. In the 1997 measurement, average quality factor remains fairly close to 1 up to a shielding depth of 1 g/cm^2, where, as with the 1991 measurement, it begins to increase. The explanation for this increase at shielding depths greater than 1 g/cm^2 most likely involves the production of high LET target fragments from nuclear interactions between trapped protons and the constituent nuclei of the detector stack. Within the range of shielding depth in the EDA, no change is expected in the LET spectrum from galactic cosmic rays. For shielding depths up to $\sim$ 1 g/cm^2 A1, the vast majority of the charged particle flux consists of trapped protons and electrons with quality factor equal to 1. At these shielding depths, the number of low-energy primary protons is much larger than the flux from secondary particles. However, as the shielding increases above 1 g/cm^2 nearly all the trapped electron flux and much of the lower energy trapped proton flux are attenuated, while at the same time there is more high-density material with which trapped protons can undergo nuclear interactions. In other words, while the flux of particles of quality factor equal to 1 decreases, the probability for production of secondaries with quality factor greater than 1 increases, leading to an increase in the average quality factor with increased shielding depth.

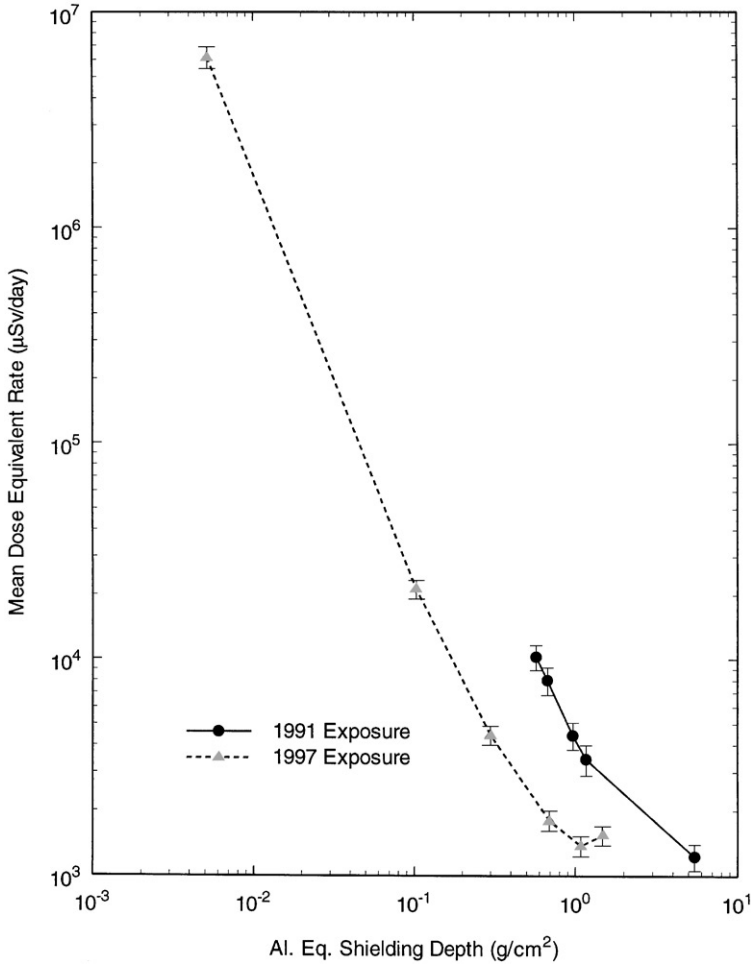

Fig. 11. Mean dose equivalent rate as a function of shielding depth in Al measured on the exterior of the Mir Kvant 2 module in 1991 and 1997.

4. Conclusions

Measurements of the mean dose and dose equivalent rates performed by our laboratory on the exterior of the Mir Orbital Station illustrate the importance of the first g/cm^2 of shielding in protecting both crew during EVA and radiation-sensitive instruments and materials from the harmful effects of the LEO space radiation environment. Mean total dose rate and mean dose equivalent rate were both seen to decrease by nearly four orders of magnitude within the first g/cm^2 of Al equivalent shielding. Most of this decrease is expected to be from the attenuation of the electron flux encountered while the spacecraft is traversing the horns of the trapped electron belts at high L values. However, as illustrated by the LET spectrum measurements made in CR-39 PNTD (which is insensitive to electrons), there is a three order of magnitude decrease in the flux of particles with $LET_{\infty}H_2O \geqslant 5$ keV/μm within the first 0.1 g/cm^2 of shielding. This decrease is due to the attenuation of low-energy trapped protons encountered in the South Atlantic Anomaly. This result has particular significance for EVA and the design of protective suits worn during EVA. While most portions of the current US and Russian EVA suits provide in excess of 0.1 g/cm^2 shielding, there may be particular areas such as around the hands where the overall shielding is considerably smaller (Shavers, 2001).

To the best of our knowledge, in this paper we are reporting three significant "firsts" in the use of passive detectors for space radiation dosimetry. This paper presents the first measurements of dose equivalent and average quality factor made on the exterior of a LEO spacecraft using passive detectors. While dose measurements using TLD have previously been carried out on the outside of LEO spacecraft, it is through the use of CR-39 PNTDs and our technique of combining the results from TLD and CR-39

Table 1
Dose and dose equivalent rates measured using CR-39 PNTDs and TLDs as a function of depth in the External Dosimeter Array exposed on the exterior of the Mir Kvant 2 module for 34 days in 1991. Low LET values are for LET < 10 keV/μm

EDA layer	Al. Eq. depth (g/cm^2)	TLD dose rate (μGy/d)	PNTD dose rate (μGy/d)	Low LET dose rate (μGy/d)	Total dose rate (μGy/d)	PNTD dose equivalent rate (μSv/d)	Total dose equivalent rate (μSv/d)	Average QF
APD	> 40	355 ± 43	46.0 ± 1.2	319 ± 40	365 ± 46	334 ± 13	653 ± 42	1.79 ± 0.25
C1-1	0.573	8726 ± 864	321.2 ± 18.7	8461 ± 977	8782 ± 1136	1814 ± 119	$10,276 \pm 1364$	1.17 ± 0.22
C1-2	0.673	5858 ± 588	338.7 ± 22.7	5586 ± 679	5924 ± 822	2409 ± 190	7995 ± 1158	1.35 ± 0.27
C1-5	0.971	2488 ± 251	266.0 ± 15.1	2278 ± 264	2544 ± 328	2149 ± 179	4429 ± 631	1.74 ± 0.33
C1-6b	1.170	1676 ± 164	298.8 ± 25.3	1436 ± 188	1735 ± 271	2004 ± 180	3440 ± 547	1.98 ± 0.44
C2-1	5.460	286 ± 29	175.3 ± 13.2	142.5 ± 15	318 ± 42	1085 ± 94	1228 ± 170	3.86 ± 0.74

Table 2
Dose and dose equivalent rates measured using CR-39 PNTDs and TLDs as a function of depth in the External Dosimeter Array exposed on the exterior of the Mir Kvant 2 module for 130.1 days in 1997. Low LET values are for LET < 10 keV/μm

EDA layer	Al. Eq. depth (g/cm^2)	TLD dose rate (μGy/d)	PNTD dose rate (μGy/d)	Low LET dose rate (μGy/d)	Total dose rate (μGy/d)	PNTD dose equivalent rate(μSv/d)	Total dose equivalent rate (μSv/d)	Average QF
APD	> 40	286 ± 13	25.6 ± 0.3	270 ± 13	295 ± 13	352 ± 4	622 ± 13	2.11 ± 0.09
1	0.0052	$6.08 \pm 0.61 \times 10^6$	$6.25 \pm 0.25 \times 10^5$	$5.56 \pm 0.60 \times 10^6$	$6.18 \pm 0.71 \times 10^6$	$6.01 \pm 0.24 \times 10^5$	$6.16 \pm 0.71 \times 10^6$	1.00 ± 0.16
2	0.1032	$2.07 \pm 0.21 \times 10^4$	270 ± 3	$2.05 \pm 0.21 \times 10^4$	$2.08 \pm 0.21 \times 10^4$	717 ± 10	$2.12 \pm 0.21 \times 10^4$	1.02 ± 0.15
4	0.299	4110 ± 410	148 ± 2	3984 ± 402	4132 ± 420	457 ± 9	4440 ± 457	1.07 ± 0.16
8	0.691	1660 ± 170	63 ± 1	1604 ± 164	1667 ± 173	201 ± 7	1805 ± 194	1.08 ± 0.16
12	1.083	1210 ± 120	65 ± 1	1153 ± 117	1218 ± 126	225 ± 7	1378 ± 146	1.13 ± 0.17
16	1.475	1050 ± 110	155 ± 2	921 ± 93	1075 ± 109	621 ± 13	1542 ± 158	1.43 ± 0.21

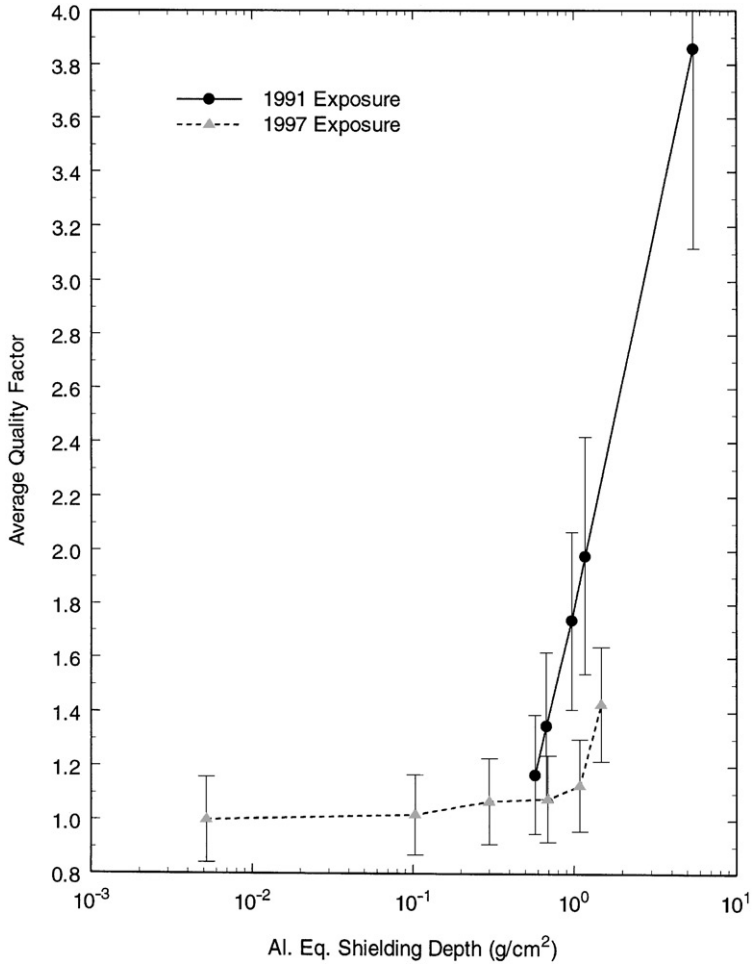

Fig. 12. Average ICRP-60 quality factor as a function of shielding depth in Al measured on the exterior of the Mir Kvant 2 module in 1991 and 1997.

PNTD measurements that makes possible the measurement of dose equivalent and average quality factor. We also present the least-shielded space measurement of an LET spectrum made to date using CR-39 PNTD and the first use of atomic force microscopy to measure LET spectrum in CR-39 PNTD exposed in space. Using conventional optical microscopy and a minimum bulk etch of ~ 8 μm, the highest track density possible in CR-39 PNTD without saturating the detector is $< 10^5$ cm^{-2} (Benton et al., 1996). With AFM, track densities in excess of 10^8 cm^{-2} are easily accommodated without track overlap. Using AFM, the duration of exposure can be greatly extended and/or the minimum shielding under which the detector is exposed can be greatly reduced. Thus, AFM permits a considerable extension in the application of PNTDs for radiation measurement in space.

References

Akatov, Yu.A., Arkhangelsky, V.V., Kovalev, E.E., Spurny, F., Votochkova, I., 1986. Absorbed dose measurements on external surface of Cosmos satellites with glass thermoluminescent detectors. Adv. Space Res. 9, 237–241.

Akatov, Yu.A., Dudkin, V.E., Kovalev, E.E., Benton, E.V., Frank, A.L., Watts Jr., J.W., Parnell, T.A., 1990. Depth distribution of absorbed dose on the external surface of Cosmos 1887 biosatellite. Nucl. Tracks Radiat. Meas. 17 (2), 105–108.

Benton, E.R., Benton, E.V., 1999. A survey of radiation measurements made aboard Russian spacecraft in low-earth orbit. NASA/CR-1999-209256.

Benton, E.R., Benton, E.V., 2001a. Space radiation dosimetry in low-Earth orbit and beyond. Nucl. Instrum. Methods B 184 (1–2), 255–294.

Benton, E.R., Benton, E.V., Frank, A.L., Frigo, L.A., Csige, I., 1996. Secondary particle contribution to the LET spectra on LDEF. Radiat. Meas. 26 (6), 793–798.

Benton, E.R., Benton, E.V., Frank, A.L., 2001b. Characterization of the radiation shielding properties of US and Russian EVA suits. Lawrence Berkeley National Laboratory Report LBNL-48977, Berkeley.

Benton, E.R., Benton, E.V., Frank, A.L., 2002. Passive dosimetry aboard the Mir Orbital Station: internal measurements. Radiat. Meas., this issue, PII: S1350-4487(02)00075-6.

Bühler, P., Desorgher, L., Zehnder, A., Daly, E., Adams, L., 1996. Observations of the low Earth orbit radiation environment from Mir. Radiat. Meas. 26 (6), 917–921.

Charvat, J., Spurny, F., Kopecka, B., Votochkova, I., 1990. Ionizing radiation fluxes and dose measurement during the Cosmos 1887 satellite flight. Nucl. Tracks Radiat. Meas. 17 (2), 109–112.

Cucinotta, F.A., 2001. NASA Johnson Space Center, private communication.

Dachev, Ts.P., Tomov, B.T., Matviichuk, Yu.N., Koleva, R.T., Semkova, J.V., Petrov, V.M., Benghin, V.V., Ivanov, Yu.V., Shurshakov, V.A., Lemaire, J.F., 1999. Solar cycle variations of Mir radiation environment as observed by the Liulin dosimeter. Radiat. Meas. 30 (1), 269–274.

Deme, S., Apathy, I., Hejja, I., Lang, E., Feher, I., 1999. Extra dose due to extravehicular activity during the NASA-4 mission measured by an on-board TLD system. Radiat. Prot. Dosim. 85 (1–4), 121–124.

Dyer, C.S., Truscott, P.R., Peerless, C.L., Watson, C.J., Evans, H.E., Knight, P., Cosley, M., Underwood, C., Cousins, T., Noulty, R., Maag, C., 1999. Implications for space radiation environment models from CREME and CREDO measurements over half a solar cycle. Radiat. Meas. 30, 569–578.

Gussenhoven, M.S., Mullen, E.G., Brautigam, D.H., 1996. Improved understanding of the Earth's radiation belts from the CRRES satellite. IEEE Trans. Nucl. Sci. 43 (2), 353–368.

International Commission on Radiological Protection, 1991. 1990 Recommendations of the International Commission on Radiological Protection. ICRP Report No. 60. Pergamon Press, Oxford.

Mitrikas, F.G., Tsetlin, V.V., 1995. Mir and other Russian spacecraft orbits examined. Kosmicheskiye Issledovaniya 33 (4), 389–394 (in Russian).

NASA, 2001. http://spaceflight.nasa.gov/station/eva/index.html

Ogura, K., Benton, E.V., Frank, A., Atallah, T., 1986. Proton response of CR-39. Nucl. Tracks Radiat. Meas. 12 (1–6), 527–530.

Schmidt, P., Fellinger, J., Hubner, K., 1990. Determination of dose distribution of cosmic radiation behind different shielding thicknesses. Nucl. Tracks Radiat. Meas. 17 (2), 117–120.

Shavers, M.R., 2001. NASA Johnson Space Center, private communication.

Shea, M.A., Smart, D.F., 1996. Solar-interplanetary phenomena in March 1991 and related geophysical and technological consequences. Radiat. Meas. 26 (3), 427–432.

Spurny, F., Votochkova, I., 1992. Depth dose behind thin shielding on the external surface of the Cosmos 2004 biosatellite. Nucl. Tracks Radiat. Meas. 20 (1), 171–173.

Stassinopoulos, E.G., 1988. The Earth's trapped and transient space radiation environment. In: McCormack, P.D., Swenborg, C.E., Bucker, H. (Eds.), Terrestrial Space Radiation and its Biological Effects, NATO ASI Series A: Life Sciences, Vol. 154. Plenum, New York.

Szabo, P.P., Feher, I., Akatov, Yu.A., Lancsarics, Gy., 1986. Dose distribution measurements in CaSO4:Dy-Teflon rods. Radiat. Prot. Dosim. 17, 212–221.

Yamamoto, M., Yasuda, N., Kurano, M., Kanai, T., Furukawa, A., Ishigure, N., Ogura, K., 1999. Atomic force microscope analyses of heavy ion tracks in CR-39. Nucl. Instrum. Methods B 152, 349–356.

Yasuda, N., Yamamoto, M., Miyahra, N., Ishigure, N., Kania, T., Ogura, K., 1998. Measurement of bulk etch rate of CR-39 with atomic force microscopy. Nucl. Instrum. Methods B 142, 111–116.